ELSEVIER_JFUE_9499

The effects of particle grinding on the burnout and surface chemistry of coals in a drop tube furnace

Julian M. Steer[a,*]

SteerJ1@cardiff.ac.uk

Richard Marsh[a,†]

David Morgan[b]

Mark Greenslade[c]

[a]Cardiff School of Engineering, Cardiff University, Queen's Buildings, The Parade, Cardiff CF24 3AA, United Kingdom

[b]Cardiff Catalysis Institute, School of Chemistry, Cardiff University, Park Place, Cardiff CF10 3AT, United Kingdom

[c]Tata steel UK, Port Talbot SA13 2NG, United Kingdom

*Corresponding author. Tel.: +44 2920870599; fax: +44 29 20874939.

~~[†]Tel.: +44 2920870599; fax: +44 29 20874939.~~

Abstract

Grinding coals to a pulverised coal specification for blast furnace injection can be costly, which is why some iron manufacturers choose a larger granulated coal size specification. However, there is a concern that these coals may have lower burnout in the raceway region so there is a technical and economic balance with coal grinding. This paper investigates how the process of grinding alters the physical properties, plus the surface chemistry, of coals and their chars formed in a drop tube furnace; it was found that in many cases the larger particle size coals gave improved combustion burnout compared to smaller sizes.

The physical properties of the chars, formed from grinding coals to different sizes, resulted in char swelling in the smaller particle sizes, compared to char fragmentation for the larger size classifications. Minerals phases associated with better coal reactivity were found to undergo higher conversion to other chemical forms with the larger size coals, suggesting a potential catalytic or synergistic contribution to their burnout. A closer look at the surface chemistry suggests that the action of grinding coals has an important effect on the surface chemistry. The XPS spectra of the chars, formed in a drop tube furnace, indicated that grinding the coals to a smaller particle size reduced the carbon–oxygen and carbon–mineral interactions compared to the larger sizes and correlated with the higher burnouts. An increasing trend was identified for the carbon sp^2 bonding with larger size and higher rank coals which correlated with their burnout at low carbon conversions; however, this did not hold at higher conversions, suggesting other factors were more dominant.

Keywords: Coal injection; XPS; Grinding; Surface properties; Drop tube furnace

1 Introduction

Coal injection is a widely established technique used in blast furnace ironmaking, but grinding the coal into a pulverised coal specification costs energy, time, and money [1]; in a study using a Western bituminous coal (Oxbow), the U.S. department for energy found there was a 60% increase in the power required to grind it to a pulverised specification [2]. For this reason some manufacturers choose a larger granulated size specification typically in the region of 100% < 2000 μm and 20% < 75 μm to save grinding costs compared to general pulverised specification of 80% < 75 μm [3–6]. However, manufacturers using granulated coal injection risk unburnt materials carrying through the furnace into the top gas and reducing the amount of coal utilised, particularly with coals that combust less well in a blast furnace raceway, such as those with lower volatile matter content [7,8]. This paper seeks to investigate the effect of particle size on the coal burnout in the context for blast furnace coal injection.

Grinding coal particles to a small particle size has been found to improve their combustion by increasing the surface area, pore volume and devolatilisation [6,9,10], but can also lead to maceral and mineral segregation effects. The maceral content of a coal affects the combustibility (temperature of combustion) and the ordering is considered to be liptinite < vitrinite < inertinite [11]. Work by Morgan et al. and Yu et al. found that burnout temperatures were reduced for smaller coal particle sizes [12,13], but the reactivity of the corresponding chars was intrinsically different due to maceral segregation effects although they were from the same coal [14]. In comparison Cloke et al. discussed this effect, noting that inertinite and fusinite

concentrate in the smaller size fractions because they are brittle compared with other macerals, but they also noted that there were exceptions to this due to maceral associations with the mineral matter [15].

Segregation of the mineral constituents by grinding coal also plays an important role as these represent the non-combustible portion of the coal; and due to their inherent hardness, increasing amounts can affect the grinding which in turn increases abrasion and wear to the milling equipment [11,16]. Studies have shown that although the highest ash levels tended to occur in the smallest size fraction this was not the same for all coals as their organic affinity varies [15,17].

Thermal fragmentation of coals is a significant effect related to particle size and composition, but limited work has been carried out relating to surface chemistry and drop tube furnace burnout [18]. Particles have been found to fragment extensively depending on the coal type, particle size, furnace temperature and volatile matter content. Dacombe et al. found that fragmentation increased with particle size and correlated with a decreasing compressive strength, while Senneca et al. and Zhang et al. identified the role of internal overpressure and higher inner pressure due to the volatile content of the larger particles and the contribution to fragmentation [9,19,20].

Some coal particles exhibit a swelling effect which has also been found to be related to particle size. It has been found that small particle sizes have high swelling [21] and that in high vitrinite bituminous coals a greater swelling effect occurred due to the higher content of this maceral, producing more char cenospheres [22]. However, although more porous chars are associated with the swollen chars, agglomeration has also been observed in some coals and may also influence burnout [10].

This paper aims to investigate reasons for differences in the burnout of coal samples, ground and classified to three different sieved particle sizes, <106 μm, <500 μm and <1000 μm, using a drop tube furnace. The different sizes had different physical properties and laser diffraction was used to measure the particle size distributions to investigate fragmentation and swelling effects related to burnout. In comparison to the state of the art, this work relates the coal burnout with the effect of grinding on the surface chemistry and physical properties using X-ray photoelectron spectroscopy (XPS) to identify bonding interactions that contribute to improvements in combustion.

2 Materials and methods

Five coal samples were milled using a TEMA™ disc mill and classified by dry sieving using the standard BS1016 109:1995 into the following three different ranges.

1. 100% < 106 μm
2. 100% < 500 μm
3. 100% < 1000 μm 50% < 250 μm

The classified samples were dried at 105 °C using BS11722:2013 until a constant weight and the volatile matter content was measured using standard BS15148:2009. Ash contents were carried out using the standard method BS 1171:2010. The petrographic maceral analysis was carried out in accordance with ISO7404 by preparing a polished particulate block and carrying out a point count under reflected light microscopy to identify the different macerals present. The samples ranged from high rank semi-anthracitic LV1 to the lower rank high volatile bituminous HV and were chosen based on their variation in proximate analyses shown in Table 1.

Table 1 Average analyses of different particle size coals (dried).

Coal type	Proximate analyses				Petrographic analyses			
	Volatile matter content (%-wt%)	Ash content (%-wt%)	Fixed carbon content (%-wt%)	Gross calorific value (MJ/kg)	Vitrinite (%-vol%)	Liptinite (%-vol%)	Inertinite (%-vol%)	Mineral matter (%-vol%)
LV1	8.2	5.8	86.0	34.6	83	1	14	2
LV2	12.5	8.6	78.9	31.9	60	0	39	1
LV3	14.4	4.7	880.9	34.2	78	1	18	3
MV	24.4	7.8	67.8	30.8	52	1	46	1
HV	33.0	6.9	60.1	31.9	71	10	17	2

A drop tube furnace (DTF) was used to characterise the devolatilisation and burnout behaviour of the coal samples at 1100 °C in air for residence times between 35 ms to and 700 ms. The high heating rate and short residence times in the DTF environment closely resemble those experienced when coal is injected into the blast air of the blast furnace raceway making this a particularly relevant technique [23–26]. Particles were fed into the top at feed rates of 30 g/hr, entrained in a laminar air flow at 20 L/min and collected at the bottom by means of a cyclone collector. The particle residence time was controlled by altering the distance of a moveable water cooled collection probe up to a maximum path length of 1.2 m from a water cooled inlet feeder.

The ash tracer method was used to calculate the burnout of the coals, sometimes referred to as the combustion efficiency [27,28]. This method assumes that the coal ash remains conserved in the char residue in the test conditions and that no ash species are volatilised. This was tested for all the coal samples at 1100 °C. It is important to note that because the burnout figures are calculated using the ash tracer method, there is room for error propagation which can lead to repeatability issues [29]. The average standard deviation for all the drop tube furnace burnouts was 2.4%, with a range from 0.1% to 4.1%.

The burnout (%) is calculated from the ash balance of the initial content of ash in the coal (A_0) and the ash content of the residue collected post DTF (A_1).

$$\text{Burnout } (\%) = \frac{10^4(A_1 - A_0)}{A_1(100 - A_0)}$$

Scanning electron microscope (SEM) images were obtained using a FEI SEM–EDX instrument XL30 ESEM FEG at 512 × 384 resolution in back scattered and secondary electron detection modes. Particle size analysis work was carried out using a Malvern Mastersizer 3000 laser diffraction particle analyser, capable of measuring between 0.01– and 3500 μm, using a wet cell accessory with obscuration levels between 4–% and 8%.

A Kratos Axis Ultra DLD system was used to collect XPS spectra using monochromatic Al X-ray source operating at 144 W. Data was collected with pass energies of 160 eV for survey spectra, and 40 eV for the high resolution scans. The system was operated in the hybrid mode, which utilises a combination of magnetic immersion and electrostatic lenses and acquired over an area approximately 300 × 700 μm. A magnetically confined charge compensation system was used to minimisze charging of the sample surface, and all spectra were taken with a 90° take off angle. A base pressure of ~1 × 10^{-9} Torr (0.133 μPa) was maintained during collection of the spectra. In all cases a binding energy of 284.5 eV was used for the C 1s peak to account for peak shifts due to differences in sample charging.

3 Results and discussion

3.1 Drop tube furnace combustion

This study was based on coal samples ground to three different particle size classifications to cover a range up to a typical granulated coal specification used by some iron manufacturers for blast furnace injection. The aim of this approach was to measure both the effect of the different particle size, and also the impact of grinding on the sample burnout.

Many studies investigating the effect of particle size are based on a ground coal that is classified by sieving to obtain a portion of a specific size fraction [15]. However, with this approach, mineral and maceral segregation can occur between the different particle sizes obtained, which can affect the combustion properties. Rather than use a selected portion of a ground sample, each sample was classified, separated, ground and reclassified. The process was repeated to meet the required particle specification and to be more representative of an industrial grinding situation, where the entire sample is used rather than a sieved portion.

The graphs shown in Fig. 1 show the relationship between the burnout and residence time through the DTF, for the five different types of coal at the three different size classifications. As expected, the wide variation in the properties of the coals was reflected in the burnouts and the order of the absolute maximum burnout correlates predictably with the order of increasing volatile matter content for the coals. Interestingly, many of the larger particle size classifications had higher burnouts than the smaller ones suggesting that either the larger sizes were more reactive or that additional grinding was detrimental to the burnout of the smaller sizes.

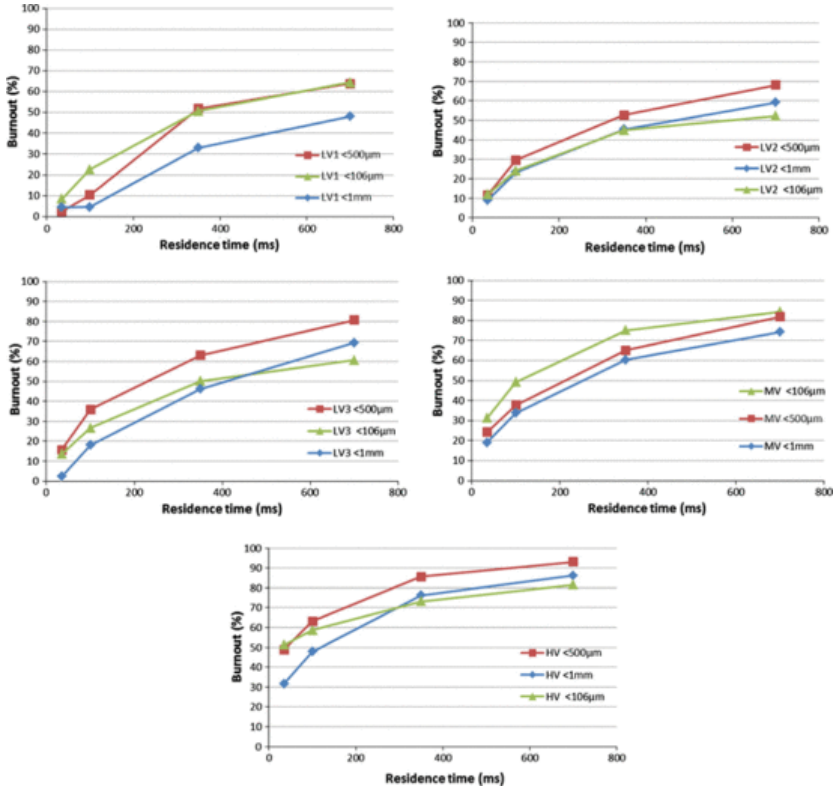

Fig. 1 Burnout of coals classified to particle sizes of 106 µm, 500 µm and 1000 µm in a DTF.

At the low DTF residence time (35 ms) the additional grinding required to meet the smaller particle size classification (<106 µm) gave negligible absolute difference in the burnout for the LV1 and LV2 low volatile content coals. For the LV3 and the HV coals, grinding to the mid-size classification of <500 µm was sufficient to give the same results as grinding and classifying to the smaller <106 µm. Only the medium volatile matter MV coal gave higher burnouts at 35 ms by grinding to the <106 µm classification at such a short residence time.

In comparison, at the higher residence time (700 ms), the <500 µm coal classification gave better burnouts for the LV2, LV3 and HV compared to the <106 µm classification. For the LV1 and MV coals the burnouts were similar for the <500 µm and <106 µm classifications. Therefore at longer residence times the results indicated that grinding to <106 µm gave little benefit to the burnouts, and with the LV2, LV3 and HV coals it had a detrimental effect.

Because of the energy requirement and cost associated with additional grinding, the results have important implications on the preparation requirements and processing of coals for blast furnace coal injection. The performance of some of the larger classifications suggests that for certain coal types, a granulated coal specification could give similar burnout performance to smaller particle size pulverised classification without the need for additional grinding.

To explain these differences in the burnout performance, the physical and chemical effects have been investigated to identify how grinding affects the coals by investigating particle swelling, fragmentation, mineral composition and surface chemistry.

3.2 Particle swelling and fragmentation effects

An important observation for the chars produced in the DTF was the variation in physical size and shape, depending on the particle size classifications of the coals from which they were derived. These changes were quantified by comparing the measured particle size distributions of the coals and the coal chars after different residence times through a drop tube furnace. It appears that the trend is for larger coal size classifications (<1000 µm) to fragment and for smaller coal size classifications (<106 µm) to swell; the coals classified to <500 µm fall somewhere in between the other classifications.

Fig. 2 compares the swelling/fragmentation of the chars produced from the different coal size classifications after 35 ms in the DTF, measured by the absolute change of the Dv90 (particle size below which 90% of the volume of sample exists). For the larger coal size classification of coal particles (<1000 µm), the LV3 and HV fragmented the most followed by the LV1 and LV2 coals. The MV coal char showed little change in the particle size at 35 ms, but for the <106 µm classification the MV and HV samples exhibited the

largest swelling effect of the measured samples.

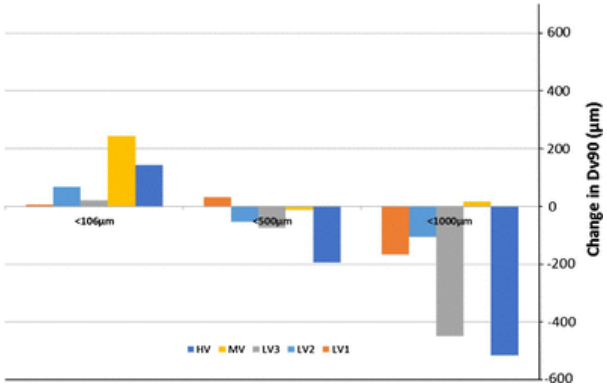

Fig. 2 Change in Dv90 of char relative to the initial coal for 35 ms residence time.

Fig. 3 compares the swelling/fragmentation effects after 700 ms in the DTF and the largest change in the chars was measured for the coals classified to <106 µm. The most significant swelling was measured for the LV3, MV and HV chars. This swelling and fragmentation effect has important implications for burnout. A swollen char is expected to have a more porous and open network allowing increased gas diffusion, while a fragmented char might be expected to have increased particle surface area with a fractured internal surface that could potentially have different surface chemistry.

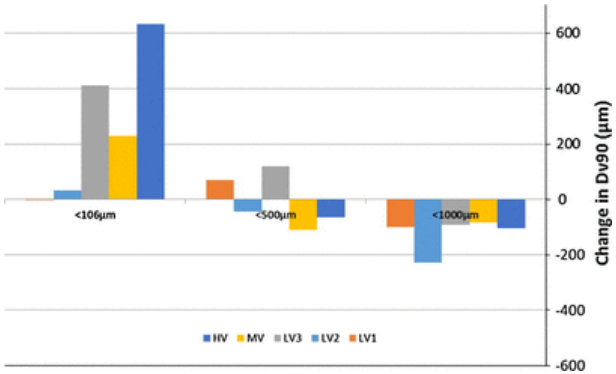

Fig. 3 Change in Dv90 for char relative to initial coal after 700 ms residence time.

Scanning electron microscope (SEM) images, shown in Figs. 4–8, were used to visualise the effect of swelling and fragmentation on cross sections of the coal char particles after 35 ms in the DTF. The char types formed from the <106 µm coal, shown in Figs. 4a, 5a, 6a, 7a, and 8a, ranged from cenospheres and network/honeycomb structures to the LV1 which had a mix of thick walled cenospherical and solid char particles as shown in Fig. 4a. In comparison, the char types shown in Figs. 4b, 5b, 6b, 7b, and 8b formed from the larger coal classification (<1000 µm) were all made up of solid particles.

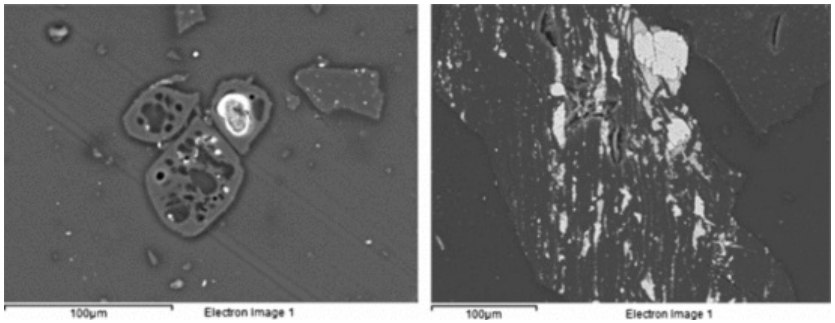

Fig. 4 Backscattered images of the LV1 char after 35 ms residence time (a) <106 µm and (b) <1000 µm.

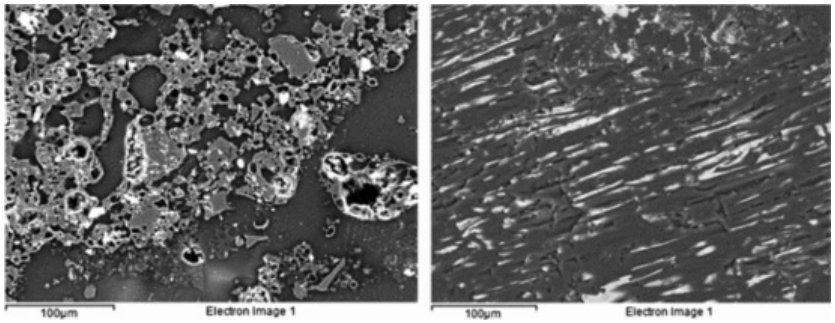

Fig. 5 Backscattered images of the LV2 char after 35 ms residence time (a) <106 µm and (b) <1000 µm.

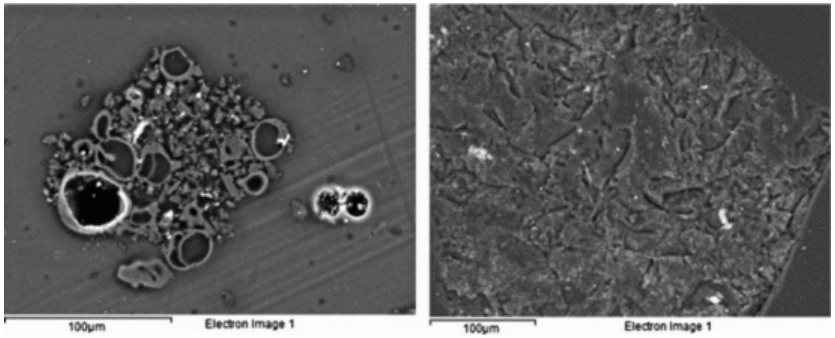

Fig. 6 Backscattered images of the LV3 char after 35 ms residence time (a) <106 µm and (b) <1000 µm.

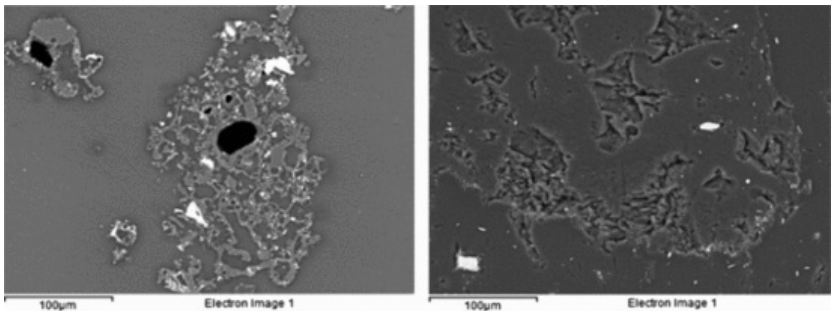

Fig. 7 Backscattered images of the MV char after 35 ms residence time (a) <106 μm and (b) <1000 μm.

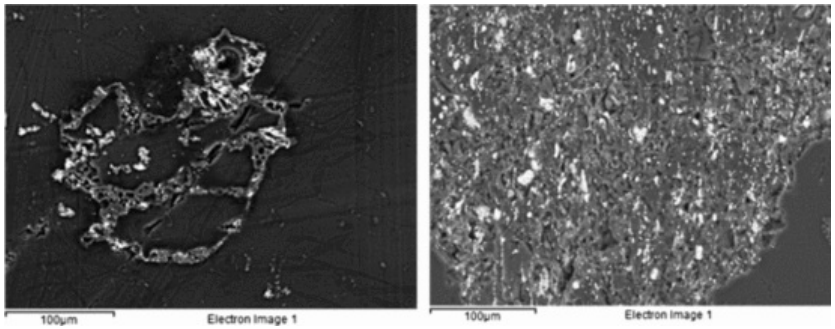

Fig. 8 Backscattered images of the HV char after 35 ms residence time (a) <106 μm and (b) <1000 μm.

Considering the magnitude of the swelling and fragmenting effect, there was no consistent correlation between the observed effects and the burnout. The overall trend after 35 ms was fragmentation of the <1000 μm classified coals, but this did not improve the burnout relative to the smaller particle size classifications. However, it might go some way to explaining why the burnout of the larger particle classifications do not differ as significantly from the small particle classification as might be expected considering the width of the particle distributions. At a residence time of 700 ms the largest effect was the char swelling, but the chars with the highest swelling showed little advantage from this effect on the burnout. The results suggest that other factors, such as the mineral composition or the surface chemistry, also play an important role on the burnout.

3.3 Mineral composition and interactions

Minerals in coal can have a catalytic, inhibitory and synergistic role on combustion and gasification and is an area that has been thoroughly researched [30–35]. Zhang et al. showed how the minerals affected the macerals and char porosity; for chars prepared in the DTF 'included minerals' facilitated the formation of pores in anthracites, but inhibited the formation of a more porous structure in bituminous coal chars [30]. Feng et al. found evidence of catalytic ordering during heat treatment depending on the mineral content. By the relation of electrical resistivity to reactivity of chars in a TGA, they suggested thermal deactivation occurred due to carbon structural ordering catalysed by the inorganic mineral matter in the coal char whereas ash-free coal chars did not vary significantly. It has also been pointed out that there is often a lack of clear and conclusive correlation about the catalytic influence of minerals, particularly combustion of high rank coals and that contradictions and uncertainties associated with the influence of mineral content could be due to inhomogeneity [33].

Coal ash samples are widely reported to contain different aluminosilicate clay mineral phases, which have been reported to produce positive combustion effects such as catalysis and negative effects such as fluxing [30–32,34–36]. In a previous paper, the authors noted differences with the surface association of minerals as inclusions, identifying them as a potential contributory factor to improvements in the burnout of some coals [37] in particular the aluminosilicate mineral illite has been identified for the formation of parallel wide pores, increasing porosity and combustibility [30,35,36].

These aluminosilicates can be present in many different phases and kaolinite is known to lose hydroxyl functionality at around 500 °C, forming metakaolin which can then undergo phase changes to form species such as mullite and cristobalite which persist as solid phases up to 1600 °C [38,39]. The changes in the mineral phases could either contribute to better burnout or conversely might be present as the result of better burnout.

Because the minerals have been shown to affect the rate of combustion, this could contribute to the increased burnout in the larger particle size coal compared to the smaller particle sizes for LV2, LV3 and HV. Table 2 shows the percentage mass of different mineral phases in the post DTF char residue calculated from their concentrations measured by XRD in the ash. The results are grouped according to the classified coal particle size used to obtain each char, and indicate changes in the mineral compositions for the char residues.

Table 2 Mineral composition (mass %) of char obtained from XRD analysis of the ash.

	Amorphous	Quartz	Illite	Mullite	Anhydrite	Corundum	Hematite	Rutile
106 μm 35 ms								
LV1	3.3	1.2	0.9	0.0	0.0	0.0	0.2	0.0
LV2	5.2	1.7	1.3	0.0	0.0	0.4	0.3	0.0

LV3	2.5	0.0	1.7	0.0	0.4	0.0	0.2	0.0
MV	7.0	2.6	0.9	0.3	0.0	0.0	0.5	0.0
HV	8.6	2.5	0.9	2.7	0.0	0.0	0.0	0.0
500 µm 35 ms								
LV1	2.5	1.2	1.3	0.0	0.0	0.0	0.2	0.0
LV2	5.3	1.7	1.2	0.0	0.0	0.3	0.2	0.0
LV3	3.8	0.0	1.3	0.0	0.5	0.0	0.2	0.0
MV	6.6	2.3	0.7	0.1	0.0	0.0	0.2	0.0
HV	7.4	2.8	1.1	0.6	0.0	0.0	0.2	0.0
106 µm 700 ms								
LV1	7.5	2.9	1.3	1.7	0.0	0.0	0.6	0.0
LV2	11.1	2.0	0.0	1.2	0.0	0.5	0.3	0.3
LV3	6.8	0.0	1.1	2.2	0.0	0.0	0.0	0.0
MV	25.6	6.5	0.0	2.5	0.0	0.0	1.4	0.0
HV	18.9	5.5	1.2	3.5	0.0	0.0	0.0	0.0
500 µm 700 ms								
LV1	9.5	2.2	0.0	2.1	0.0	0.0	0.0	0.0
LV2	14.6	2.6	0.0	2.4	0.0	1.3	0.4	0.4
LV3	15.8	0.0	0.0	4.2	0.0	0.0	1.1	0.0
MV	21.9	4.4	0.0	4.1	0.0	0.0	0.9	0.0
HV	32.4	11.6	0.0	6.6	0.0	0.0	0.0	0.0

In particular, the illite mineral phase present in the <106 µm and <500 µm chars at low 35 ms residence time decreases when held at the 700 ms residence time. For the <106 µm coals it was absent from the LV2 and MV char, but for the <500 µm particle classification it was completely absent for all the coal chars. The results suggest that the illite either converts to another phase or combines to form a non-crystalline amorphous phase and that this occurs more readily for the larger <500 µm particle size coals. Considering the role that the potassium (contained in the illite) has been shown to improve combustion in coal, this conversion/consumption could be a contributing factor to the better burnouts for some of the coals at <500 µm.

Apart from the low levels in MV and HV, the mullite mineral phase absent in the <106 µm chars and the <500 µm chars at 35 ms was present at higher levels after 700 ms, and particularly for the larger <500 µm coal particle size. Fig. 9 plots the change in the mullite as the absolute percentage in the char (calculated using the char ash content and the mullite concentration measured by XRD in the ash) against burnout. An increasing trend in the mullite contained in the char correlates with increasing burnout and suggests that it may either play a role in catalysing burnout or that is indicates the conversion of other mineral phases which might have a role increasing the burnout.

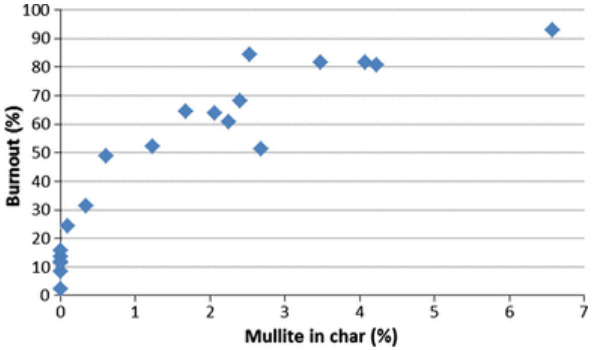

Fig. 9 Sample burnout plotted against the concentration of mullite in the char residue.

3.4 Surface chemistry analysis using X-ray photoelectron spectroscopy (XPS)

The previous section used bulk analysis techniques to investigate sample changes, but the interfacial gas–solid reaction is fundamental in coal combustion, herein we investigate the surface chemistry using XPS, which looks specifically at the coal surface to a depth of circa 10 nm [40]. A valuable aspect of this technique is the information that it gives regarding the surface chemistry and this has been used previously for coal research to compare the effect of rank, ash mineral associations, and the effect of weathering on the surface of coals [32,41–44].

The carbon spectral peaks are made up of chemical information which can be deconvoluted by peak fitting to determine carbon–oxygen bonding and carbon hybridisation. This involves the separation of overlapping peak intensities by constructing a peak model from known line-shapes and fitting these synthetic component peaks to the peak data envelope. However, it is well recognised that there is some difficulty in this technique due to C 1s peak asymmetry which affects peak fitting [45–48] and this should be considered in the findings. Coal is a highly heterogeneous material and the high resolution spectra of the C 1s region indicate a range of different carbon–oxygen bonding present on the sample surface which shift the electron binding energies (BE) depending on the chemical environments surrounding the carbons [48]. These shifts can be problematic to accurately determining the split between carbon sp^2 and sp^3 bonding areas by the peak deconvolution method which is why we have also used the C KLL Auger spectra to determine the carbon hybridisation more accurately [49].

Table 3 details the peak fitting figures for the carbon spectra which were deconvoluted into five component peaks corresponding to graphitic sp^2 type carbon bonding (peak I BE = 284.3–284.5 eV); sp^3 type carbon bonding (peak II BE = 285.1–285.5 eV); carbon present in alcohol or ether groups (peak III BE = 285.6–286.5 eV); carbonyl groups (peak IV BE = 287.0–287.8 eV); and carboxyl or ester functions (peak V BE = 288.1–288.8 eV) [42,43,50–53]. Other peaks were also recorded and those at binding energies greater than 290 eV are usually attributed to π–π* aromatic shake up effects, while those below 284 eV are attributed to plasmon loss features in this region. However, it should be noted that the peaks in the 289.4–290.9 eV range have been associated with multiple oxygen bonding in carbonate and anhydride structures identified by Beamson and Briggs in polymers [53]; their work also identified carbidic bonding in some samples around 283 eV, attributable to the metal–carbon bonding associated with the mineral content in the LV1, LV2 and HV chars derived from the larger particle coal classifications.

Table 3 Absolute atomic % of deconvoluted high resolution XPS C 1s spectra.

Peak	I	II	III	IV	V	Satellite π–π* peaks			C 1s
Binding energy range (eV)	284.3–284.5	285.1–285.5	285.6–286.5	287.0–287.8	288.1–288.8	289.4–290.9	291.2–292.1	293.4–293.9	Total %
LV1 coal									
106 µm	49.7	11.0	4.3	–	–	2.2	–	0.6	67.8
500 µm	56.3	13.0	3.3	–	1.4	2.2	–	0.5	76.8
1000 µm	58.9	5.7	3.7	–	1.6	2.7	–	0.7	73.5
LV1 char									
106 µm 700 ms	43.8	16.3	4.7	–	2.4	1.6	–	–	68.8

500 µm 700 ms	41.3	15.2	12.3	–	5.2	1.9	1.5	–	77.4
1000 µm 700 ms	42.4	21.4	6.2	–	6.6	1.8	1.5	–	79.9
LV2 coal									
106 µm	72.7	9.4	1.9	–	1.5	0.3	–	–	85.8
500 µm	56.0	14.3	4.4	–	2.5	0.7	–	–	78.0
1000 µm	50.2	17.0	4.9	–	1.9	0.7	–	–	74.7
LV2 char									
106 µm 700 ms	54.6	16.9	8.1	–	2.3	0.3	–	–	82.2
500 µm 700 ms	42.1	17.7	19.0	2.6	2.7	1.1	–	–	85.3
1000 µm 700 ms	53.5	12.1	11.2	5.4	–	2.7	–	–	84.9
HV coal									
HV 106 µm	40.2	19.0	4.9	1.8	1.2	1.5	–	–	68.5
HV 500 µm	35.6	11.1	11.2	6.1	1.8	–	–	–	65.9
HV 1000 µm	36.3	13.1	5.9	8.3	1.6	0.8	–	–	66.1
HV char									
106 µm 700 ms	45.7	18.5	10.2	2.0	3.2	1.3	–	–	80.9
500 µm 700 ms	43.7	3.8	1.6	13.7	5.4	3.6	–	2.3	74.1
1000 µm 700 ms	38.6	19.8	–	20.7	3.2	3.7	–	–	86.0

The high resolution scans revealed detailed information on the carbon (C 1s) peaks, looking specifically at the changes caused by grinding and related to the burnout. Work by other authors, has identified the importance of surface oxygen species on the reactivity; Cope et al. noted that below 1200 °C the formation of surface oxides inhibits the structural anisotropy and enhances reactivity [54], and Wan et al. noted that the mineral composition of the coals activates the early stage carbon gasification by acting as an oxygen shuttling agent [32].

3.4.1 High resolution C 1s spectra – coals

The C 1s spectra of the high rank semi-anthracitic LV1 coal in Fig. 10, shows little difference in the absolute quantity of C—O bonding for the different particle size classifications which ranged from 4.3% –to 5.3%. However the LV2 in Fig. 11, and particularly the lower rank HV coal in Fig. 12, both had higher measured concentrations in the larger particle size classifications which had undergone less grinding. Both showed asymmetrical peak broadening in the higher binding energy region associated with carbon–oxygen bonding as ether groups (C—O) and ester groups (O═C—O), ranging from 3.4% –to 6.9% in the LV2 and from 7.9% –to 19.1% for the HV coal, which also included carbonyl (C═O) bonding.

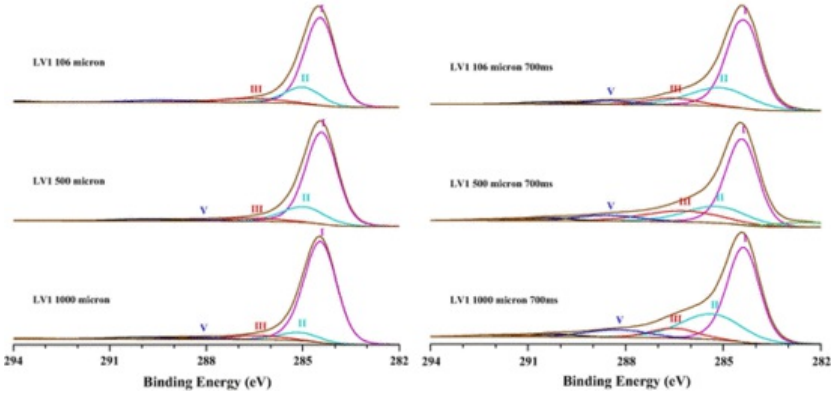

Fig. 10 XPS deconvoluted C 1s spectra for particle size classifications of LV1 (a) coal and (b) char.

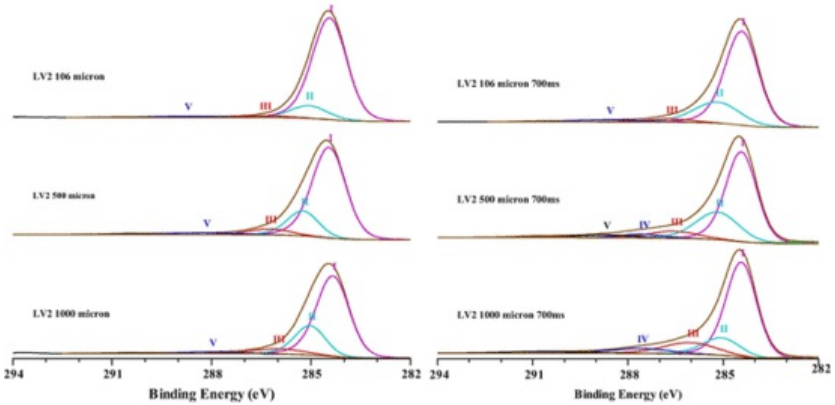

Fig. 11 XPS deconvoluted C 1s spectra for particle size classifications of LV2 (a) coal and (b) char.

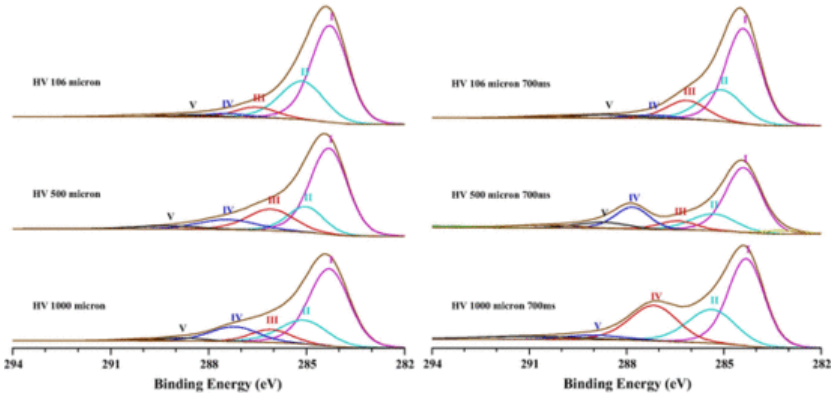

Fig. 12 XPS deconvoluted C 1s spectra for particle size classifications of HV (a) coal and (b) char.

3.4.2 High resolution C 1s spectra – chars

Compared to the coals, the spectra for the chars obtained after a burnout residence time of 700 ms had greater peak asymmetry with significant peak shoulders in the higher binding energy region, associated with more carbon–oxygen bonding. The results suggest that the physical process of grinding the coal changes the surface chemistry; either by reducing the number of reactive functional groups, or due to the physical effects associated with different particle size. The trend observed previously in Figs. 2 and 3, was for smaller coal particles to swell and the larger particles to fragment, and it is the latter effect which could influence the surface chemistry and reactivity by exposing cleaved surfaces not subjected to the mechano-chemical effects caused by grinding.

Fig. 10 shows the peak fitted spectra for the LV1 chars and indicates higher levels of C—O bonding in the form of ether and ester groups, ranging from 7.1–% to 17.5%, compared to the LV1 coals from which they were derived. The LV2 char, shown in Fig. 11, also shows peak broadening for all the particle classifications compared to the coals and it is the larger particle sizes that have the greater concentration ranging from 10.4%– to 24.3%.

The most pronounced peak profile changes were observed in the HV char, shown in Fig. 12, which exhibited a bimodal shape for the <500 μm and <1000 μm particle sizes and C—O bonding concentrations ranging from 15.4% in the smallest 106 μm classification to 23.9% in the largest 1000 μm.

3.4.3 Carbon Auger electron spectroscopy

Issues regarding the accuracy of the peak fitting technique for the determination of the carbon hybridisation from the C 1s peak have been widely discussed and other authors have recognised particular difficulties differentiating the subtle differences between sp^2 and sp^3 signals. These are made worse with highly asymmetric peak shapes in hydrogenated samples such as those encountered with heterogeneous coal samples [45–48].

An alternative technique to determine the sp^2/sp^3 carbon hybridisation using the X-ray excited Carbon Auger (C_{KLL}) spectra was originally reported by Lascovich et al.and Scaglione by measuring the distance, *D*, between the positive and negative peaks of the first derivative of the spectrum [55]. A linear approximation was proposed ranging from diamond at $D = 14.2$ eV, in which the carbons are 100% in the sp^3 configuration, to graphite at 22.5 eV where the carbons are 100% in the sp^2 configuration. In this range Lascovich et al. also measured the sp^2/sp^3 ratio of samples of amorphous carbon and hydrogenated amorphous carbon samples and since then other authors have extended this investigation to other forms of carbon such as carbonised wood, which include up to 21% oxygen bound on the surface and still show a linear relationship [47].

It has been previously noted by Leung et al. and Yan et al. that the sp^2/sp^3 values obtained from the *D*-parameter are consistently smaller than those values obtained using the peak fitting method and this is true for these results too. This is thought to be due to the influence of secondary electron emission on the auger peak [48,49,56] and Lascovich et al. found that an increase of the hydrogen content in hydrogenated amorphous carbon films corresponded to an increase in the sp^3 content.

The Cearbon aAuger data for the coal samples (Table 4) shows a maximum sp^2 percentage of 20.8% in the semi anthracitic LV1 coal, 9.0% in the low volatile bituminous LV2, and 0% in the HV corresponding to different degrees of coalification from the high rank to lower rank.

Table 4 XPS Carbon Auger (C_{KLL}) *D* parameter and sp^2 bonding character of coal samples.

	D (eV)	% sp^2 (absolute)
Graphite[a]	22.5	–
Diamond[a]	14.3	–
LV1 106 μm	14.2	0.0
LV1 500 μm	15.1	8.2
LV1 1000 μm	16.5	20.8
LV2 106 μm	14.2	0.0
LV2 500 μm	14.6	3.5
LV2 1000 μm	15.2	9.0
HV 106 μm	14.4	1.3
HV 500 μm	14.2	0.0
HV 1000 μm	14.4	1.3

[a] Lascovich et al. [+55].

The sp^2 π-bonding corresponds to resonance stabilised aromatic/double bond character found in graphitic type structurally ordered carbon bonding. The results however, suggest that the predominant bonding in the coal measured using XPS is sp^3, the type of sigma bonding associated with single covalent bonds in aliphatic compounds. Grinding the coals to smaller particle size correlated with a reduction in the sp^2 character corresponding to bond cleavage of the carbon which changes the surface chemistry. This is most relevant to the LV1 coal with 28.3% sp^2 character for the <1000 μm particle size as grinding this to <106 μm gave a much improved burnout profile compared to grinding the other coals.

The results in Table 5 show the measured percentage sp^2 character of the coal chars after 700 ms residence time in the DTF. Compared to the coals from which they were derived, the chars have higher sp^2 aromatic/double bond character. The increase suggests thermal structural ordering of the carbons related to the sp^2 bonding found in highly ordered graphitic carbon, previously observed in the literature and which has been correlated to reductions in char reactivity [57–59]. Additionally, the preferential combustion of the more reactive and less ordered sp^3 bonded aliphatic carbons results in higher concentrations of the sp^2 bonded carbons present at the surface of the char.

Table 5 XPS Carbon Auger (C_{KLL}) *D* parameter and sp^2 bonding character of coal char samples (700 ms).

	D (eV)	% sp^2(absolute)	% DTF burnout after 35 ms	% DTF burnout after 700 ms
LV1 106 μm	16.4	18.6	8.5	64.5
LV1 500 μm	17.8	34.5	2.4	63.9
LV1 1000 μm	18.4	41.6	4.4	48.1
LV2 106 μm	14.3	0.6	11.9	52.3
LV2 500 μm	15.4	12.4	11.6	68.1
LV2 1000 μm	16.0	18.7	9.0	59.2
HV 106 μm	14.8	5.7	51.3	81.6
HV 500 μm	15.1	7.9	48.8	93.0
HV 1000 μm	15.5	13.5	31.7	86.2

The smaller particle size classifications of each coal char (Table 5) had lower sp^2 character compared to the larger classifications and correspondingly higher char burnout at low residence time in the DTF. This relative trend was also reflected with an improved burnout with a lower rank of coal (HV > LV2 > LV1). This is consistent with other work such as Lu et al. who showed a relationship with increasing aromaticity and decreasing char reactivity [60]. However the results indicate no direct correlation between the absolute quantity of sp^2 character for each of the coals and burnout.

Also, there is no such correlation between burnout at higher levels of carbon conversion and the sp^2 character. This suggests other variables such as particle swelling, fragmentation, or the type of surface oxygen bonding are likely to play a dominant role in the reactivity compared to the carbon bonding at higher conversion levels.

4 Conclusion

The results suggest that, in addition to the importance of size on coal particle burnout, the process of grinding alters the physical properties and surface chemistry so that in some cases the larger size classifications give improved combustion burnout profiles compared to smaller sizes.

Physical changes to the particle behaviour occurred on grinding where the smallest particle size coals exhibited particle swelling on combustion producing cenospherical and network chars, whereas the larger classifications resulted in fragmented solid chars. The presence of minerals such as illite has been demonstrated by many authors to play an important role in improved combustion of coal, and in most cases in this study, the larger particles resulted in higher conversion of the aluminosilicate minerals mullite and illite. Combined with the trend of increasing burnout with increasing mullite levels there is a suggestion that these changes may indicate a catalytic or synergistic role, although it cannot be discounted that they were the consequence of burnout.

The interaction of oxygen and carbon is fundamental to the surface chemistry of combustion and the larger particle sizes had a wider variety of oxygen–carbon bonding on the char surfaces compared to smaller ones. This positive effect

could be related to the particle fragmentation exposing 'cleaved' surfaces which were more reactive.

Other authors have linked sp^2 bonding with structural ordering and reduced reactivity; analysis of the eCarbon eAuger peak indicated that the coals had up to 20.8% sp^2 bonding which reduced on grinding. However, the sp^2 content increased for the chars, compared to the coals from which they were derived, which was related to the coal particle size and to increasing rank of coal. At lower levels of carbon conversion these higher levels of the sp^2 bonding correlated with reduced burnout, but at higher carbon conversion other variables were more dominant.

Acknowledgement

The authorship wishes to acknowledge and thank Tata Steel Europe Ltd. for financial assistance with this project and support obtaining samples.

References

[1]

H. Guo, B. Su, J. Zhang, J. Shao, H. Zuo and S. Ren, Energy conservation for granular coal injection into a blast furnace, *JOM* **64**, 2012, 1002–1010.

[2]

U.S.D.o. Energy, Blast furnace granulated coal injection system demonstration project, 2000, National Energy Technology Laboratory; P.O. Box 880, 3610 Collins Ferry Road Morgantown, WV 26507-0880.

[3]

D. Osborne, The coal handbook: towards cleaner production, 2013, Woodhead Publishing.

[4]

Maldonado R, Hanniker G, Pettifor M. Granular coal injection into blast furnaces at the scunthorpe works of the british steel corporation. In: Proceedings – ironmaking conference; 1985. p. 425–35.

[5]

D.G. Hill, L.E. Makovsky, T.A. Sarkus and H.G. McIlvried, Blast furnace granular coal injection at Bethlehem Steel's Burns Harbor Plant, *Miner Process Extract Metall Rev* **25**, 2004, 49–65.

[6]

R. Barranco, M. Colechin, M. Cloke, W. Gibb and E. Lester, The effects of pf grind quality on coal burnout in a 1 MW combustion test facility, *Fuel* **85**, 2006, 1111–1116.

[7]

C. Moon, Y. Sung, S. Ahn, T. Kim, G. Choi and D. Kim, Thermochemical and combustion behaviors of coals of different ranks and their blends for pulverized-coal combustion, *Appl Therm Eng* **54**, 2013, 111–119.

[8]

S. Raygan, H. Abdizadeh and A.E. Rizi, Evaluation of four coals for blast furnace pulverized coal injection, *J Iron Steel Res Int* **17**, 2010, 8–12, 20.

[9]

H. Zhang, K. Cen, J. Yan and M. Ni, The fragmentation of coal particles during the coal combustion in a fluidized bed, *Fuel* **81**, 2002, 1835–1840.

[10]

W.H. Chen, S.W. Du and T.H. Yang, Volatile release and particle formation characteristics of injected pulverized coal in blast furnaces, *Energy Convers Manage* **48**, 2007, 2025–2033.

[11]

I.-R. Suarez and J.C. Crelling, Applied coal petrology: the role of petrology in coal utilisation, 2008, Academic Press.

[12]

P.A. Morgan, S.D. Robertson and J.F. Unsworth, Combustion studies by thermogravimetric analysis. 1. Coal oxidation, *Fuel* **65**, 1986, 1546–1551.

[13]

D. Yu, M. Xu, J. Sui, X. Liu, Y. Yu and Q. Cao, Effect of coal particle size on the proximate composition and combustion properties, *Thermochim Acta* **439**, 2005, 103–109.

[14]

P.A. Morgan, S.D. Robertson and J.F. Unsworth, Combustion studies by thermogravimetric analysis. 2. Char oxidation, *Fuel* **66**, 1987, 210–215.

[15]

M. Cloke, E. Lester and A. Belghazi, Characterisation of the properties of size fractions from ten world coals and their chars produced in a drop-tube furnace, *Fuel* **81**, 2002, 699–708.

[16]

S. Ural and M. Akiylidz, Studies of the relationship between mineral matter and grinding properties for low-rank coals, *Int J Coal Geol* **60**, 2004, 81–84.

[17]

F.E. Huggins, Overview of analytical methods for inorganic constituents in coal, *Int J Coal Geol* **50**, 2002, 169–214.

[18]

G. Liu, H. Wu, R.P. Gupta, J.A. Lucas, A.G. Tate and T.F. Wall, Modeling the fragmentation of non-uniform porous char particles during pulverized coal combustion, *Fuel* **79**, 2000, 627–633.

[19]

O. Senneca, M. Urciuolo, R. Chirone and D. Cumbo, An experimental study of fragmentation of coals during fast pyrolysis at high temperature and pressure, *Fuel* **90**, 2011, 2931–2938.

[20]

P. Dacombe, M. Pourkashanian, A. Williams and L. Yap, Combustion-induced fragmentation behavior of isolated coal particles, *Fuel* **78**, 1999, 1847–1857.

[21]

J. Yu, J. Lucas, V. Strezov and T. Wall, Swelling and char structures from density fractions of pulverized coal, *Energy Fuels* **17**, 2003, 1160–1174.

[22]

D. Yu, M. Xu, X. Liu and Q. Cao, Swelling characteristics of coal chars and formation of residual ash particles, *Huazhong Keji Daxue Xuebao (Ziran Kexue Ban)/J Huazhong Univ Sci Technol (Nat Sci Ed)* **34**, 2006, 101–104.

[23]

M.L. Chan, J.M. Jones, M. Pourkashanian and A. Williams, Oxidative reactivity of coal chars in relation to their structure, *Fuel* **78**, 1999, 1539–1552.

[24]

S.W. Du, W.H. Chen and J.A. Lucas, Pulverized coal burnout in blast furnace simulated by a drop tube furnace, *Energy* **35**, 2010, 576–581.

[25]

H. Li, L. Elliott, H. Rogers, P. Austin, Y. Jin and T. Wall, Reactivity study of two coal chars produced in a drop-tube furnace and a pulverized coal injection rig, *Energy Fuels* **26**, 2012, 4690–4695.

[26]

J. Steer, R. Marsh, A. Griffiths, A. Malmgren and G. Riley, Biomass co-firing trials on a down-fired utility boiler, *Energy Convers Manage* **66**, 2013, 285–294.

[27]

T.R. Ballantyne, P.J. Ashman and P.J. Mullinger, A new method for determining the conversion of low-ash coals using synthetic ash as a tracer, *Fuel* **84**, 2005, 1980–1985.

[28]

W.-H. Chen, S.-W. Du, C.-H. Tsai and Z.-Y. Wang, Torrefied biomasses in a drop tube furnace to evaluate their utility in blast furnaces, *Bioresour Technol* **111**, 2012, 433–438.

[29]

E. Biagini and M. Marcucci, Review of methodologies for coal characterisation, 2000, International Flame Research Foundation.

[30]

H. Zhang, W.X. Pu, S. Ha, Y. Li and M. Sun, The influence of included minerals on the intrinsic reactivity of chars prepared at 900 °C in a drop tube furnace and a muffle furnace, *Fuel* **88**, 2009, 2303–2310.

[31]

Pohl JH. Influence of mineral matter on the rate of coal char combustion. In: ACS symposium series; 1986. p. 430–6.

[32]

Shaolong Wan, Wei-Yin Chen and Guang Shi, Roles of mineral matter in the early stages of coal combustion, *Energy Fuels* **23**, 2009, 710–718.

[33]

S. Gupta, Y. Al-Omari, V. Sahajwalla and D. French, Influence of carbon structure and mineral association of coals on their combustion characteristics for Pulverized Coal Injection (PCI) application, *Metall Mater Trans B: Process Metall Mater Process Sci* **37**, 2006, 457–473.

[34]

Z. Wei, J. Michael Moldowan, J. Dahl, T.P. Goldstein and D.M. Jarvie, The catalytic effects of minerals on the formation of diamondoids from kerogen macromolecules, *Org Geochem* **37**, 2006, 1421–1436.

[35]

R. Menendez, D. Alvarez, A.B. Fuertes, G. Hamburg and J. Vleeskens, Effects of clay minerals on char texture and combustion, *Energy Fuels* **8**, 1994, 1007–1015.

[36]

D.A. Spears, Role of clay minerals in UK coal combustion, *Appl Clay Sci* **16**, 2000, 87–95.

[37]

J.M. Steer, R. Marsh, M. Greenslade and A. Robinson, Opportunities to improve the utilisation of granulated coals for blast furnace injection, *Fuel* 2014.

[38]

A.P. Reifenstein, H. Kahraman, C.D.A. Coin, N.J. Calos, G. Miller and P. Uwins, Behaviour of selected minerals in an improved ash fusion test: quartz, potassium feldspar, sodium feldspar, kaolinite, illite, calcite, dolomite, siderite, pyrite and apatite, *Fuel* **78**, 1999, 1449–1461.

[39]

I. Suárez-Ruiz and J.C. Crelling, Applied coal petrology: the role of petrology in coal utilization, 2008, Academic Press.

[40]

C. XPS. CASA XPS Manual; 2013.

[41]

B. Gong, P.J. Pigram and R.N. Lamb, Surface studies of low-temperature oxidation of bituminous coal vitrain bands using XPS and SIMS, *Fuel* **77**, 1998, 1081–1087.

[42]

W. Geng, Y. Kumabe, T. Nakajima, H. Takanashi and A. Ohki, Analysis of hydrothermally-treated and weathered coals by X-ray photoelectron spectroscopy (XPS), *Fuel* **88**, 2009, 644–649.

[43]

R. Pietrzak, T. Grzybek and H. Wachowska, XPS study of pyrite-free coals subjected to different oxidizing agents, *Fuel* **86**, 2007, 2616–2624.

[44]

W. Xia, J. Yang and C. Liang, Investigation of changes in surface properties of bituminous coal during natural weathering processes by XPS and SEM, *Appl Surf Sci* **293**, 2014, 293–298.

[45]

R.A.P. Smith, C.W. Armstrong, G.C. Smith and P. Weightman, Observation of a surface chemical shift in carbon 1s core-level photoemission from highly oriented pyrolytic graphite, *Phys Rev B – Condens Matter Mater Phys* **66**, 2002, 2454091–2454096.

[46]

K.C. Prince, I. Ulrych, M. Peloi, B. Ressel, V. Cháb, C. Crotti, et al., Core-level photoemission from graphite, *Phys Rev B – Condens Matter Mater Phys* **62**, 2000, 6866–6868.

[47]

A. Mezzi and S. Kaciulis, Surface investigation of carbon films: from diamond to graphite, *Surf Interface Anal* **42**, 2010, 1082–1084.

[48]

T.Y. Leung, W.F. Man, P.K. Lim, W.C. Chan, F. Gaspari and S. Zukotynski, Determination of the sp3/sp2 ratio of a-C: H by XPS and XAES, *J Non-Cryst Solids* **254**, 1999, 156–160.

[49]

B.J. Jones and J.J. Ojeda, Substrate and material transfer effects on the surface chemistry and texture of diamond-like carbon deposited by plasma-enhanced chemical vapour deposition, *Surf Interface Anal* **44**, 2012, 1187–1192.

[50]

S. Biniak, G. Szymański, J. Siedlewski and A. Światkoski, The characterization of activated carbons with oxygen and nitrogen surface groups, *Carbon* **35**, 1997, 1799–1810.

[51]

S.D. Gardner, C.S.K. Singamsetty, G.L. Booth, G.R. He and C.U. Pittman, Jr., Surface characterization of carbon fibers using angle-resolved XPS and ISS, *Carbon* **33**, 1995, 587–595.

[52]

B. Gong, P.J. Pigram, R.N. Lamb and C.R. Ward, Surface characterisation of mineral matter in an Australian bituminous coal (Whybrow seam, NSW) using X-ray photoelectron spectroscopy and laser ionisation mass analysis, *Fuel Process Technol* **50**, 1997, 69–86.

[53]

G. Beamson and D. Briggs, High resolution XPS of organic polymers – the scienta ESCA300 database, 1992, John Wiley & Sons.

[54]

R.F. Cope, C.B. Arrington and W.C. Hecker, Effect of CaO surface area on intrinsic char oxidation rates for Beulah Zap chars, *Energy Fuels* **8**, 1994, 1095–1099.

[55]

J.C. Lascovich and S. Scaglione, Comparison among XAES, PELS and XPS techniques for evaluation of Sp2 percentage in a-C:H, *Appl Surf Sci* **78**, 1994, 17–23.

[56]

X.B. Yan, T. Xu, S.R. Yang, H.W. Liu and Q.J. Xue, Characterization of hydrogenated diamond-like carbon films electrochemically deposited on a silicon substrate, *J Phys D: Appl Phys* **37**, 2004, 2416–2424.

[57]

L. Lu, V. Sahajwalla and D. Harris, Coal char reactivity and structural evolution during combustion-factors influencing blast furnace pulverized coal injection operation, *Metall Mater Trans B: Process Metall Mater Process Sci* **32**, 2001, 811–820.

[58]

B. Feng, S.K. Bhatia and J.C. Barry, Structural ordering of coal char during heat treatment and its impact on reactivity, *Carbon* **40**, 2002, 481–496.

[59]

N.V. Russell, J.R. Gibbins and J. Williamson, Structural ordering in high temperature coal chars and the effect on reactivity, *Fuel* **78**, 1999, 803–807.

[60]

L. Lu, C. Kong, V. Sahajwalla and D. Harris, Char structural ordering during pyrolysis and combustion and its influence on char reactivity, *Fuel* **81**, 2002, 1215–1225.

Highlights

- Some larger coal particle sizes had better burnouts than smaller sizes.
- More surface oxygen bonding on the chars of larger particles compared to smaller ones.
- Grinding reduced sp^2 carbon bonding correlating with better burnout at low conversion.
- Smaller particle size coals tend to swell while larger size coals tend to fragment.
- More mineral phase changes occurred in the larger size coals.

Queries and Answers

Query: Your article is registered as a regular item and is being processed for inclusion in a regular issue of the journal. If this is NOT correct and your article belongs to a Special Issue/Collection please contact aravind.kumar@elsevier.com immediately prior to returning your corrections.
Answer: Regular item.

Query: Please confirm that given name(s) and surname(s) have been identified correctly.
Answer: Correct

Query: The country name has been inserted for the affiliations ‘b and c’. Please check, and correct if necessary.
Answer: Correct

Query: Please check whether the designated corresponding author is correct, and amend if necessary.
Answer: Correct. Corresponding author Julian M Steer

Query: Please check the edit(s) made in the sentence ‘Table 3 details the peak fitting figures...’, and correct if necessary.
Answer: Correct

Query: Please check the hierarchy of the section headings.
Answer: Correct

Query: Please check the author names in Refs. [32,39,53].
Answer: Correct

Query: The partfigure labels are provided in captions but not mentioned in artwork of Figs. 4–8 and 10–12. Please check and correct.
Answer: Correct and format consistent with a previous FUEL article by author

Query: In citation author name ‘Lascovich et al. [1]’ does not match with the list. Please check, and correct if necessary.
Answer: Corrected